Journal of Experimental Marine Biology and Ecology 466 (2015) 110–119

Contents lists available at ScienceDirect

Journal of Experimental Marine Biology and Ecology

journal homepage: www.elsevier.com/locate/jembe

Effects of salinity changes on coastal Antarctic phytoplankton physiology and assemblage composition

M. Hernando [a,*], I.R. Schloss [b,c,d], G. Malanga [e], G.O. Almandoz [c,f], G.A. Ferreyra [d], M.B. Aguiar [a], S. Puntarulo [e]

[a] Departamento de Radiobiología, Comisión Nacional de Energía Atómica, Buenos Aires, Argentina
[b] Instituto Antártico Argentino, Argentina
[c] CONICET, Buenos Aires, Argentina
[d] Institut des sciences de la mer de Rimouski, Rimouski, Quebec, Canada
[e] Physical-Chemistry, Institute of Biochemistry and Molecular Medicine (IBIMOL), School of Pharmacy and Biochemistry, University of Buenos Aires - CONICET, Argentina
[f] División Ficología, Facultad de Ciencias Naturales y Museo, Universidad Nacional de La Plata, La Plata, Argentina

ARTICLE INFO

Article history:
Received 14 August 2014
Received in revised form 13 February 2015
Accepted 14 February 2015
Available online xxxx

Keywords:
Antarctica
DCFH-DA
Diatoms
Meltwater
αT
βC

ABSTRACT

A natural marine phytoplankton assemblage from a coastal environment of Antarctica was experimentally exposed to low salinity sea water (30 vs 34 in the control) during 8 days in order to study their physiological and community responses to hypoosmotic stress conditions. Hypoosmotic conditions favour water influx into the cells, which results in increased turgor pressure and increased oxidative stress. This stress is linked to a number of other cellular toxic processes, including damages to proteins, enzyme inactivation and DNA breakage. Inhibition of the instantaneous growth rate started after 48 h exposure to low salinity, but at the end of experiment, growth was significantly higher in the low than in the normal (control) salinity treatment. Hypoosmotic conditions prevented phytoplankton biomass accumulation, as evidenced by reduced Chlorophyll-a concentrations as compared to the control treatment. However, in terms of cell numbers and species composition, we observed a gradual replacement of big centric by small pennate diatoms, which became dominant by the end of the experiment. In addition, the content of reactive oxygen species (ROS) and 2-thiobarbituric acid-reactive substances (TBARS), which are indicative of oxidative stress, were studied. In the low salinity treatments, ROS concentrations were significantly higher than control values on days 4 and 6, decreasing thereafter to nearly initial values. TBARS content increased during the first 48 h and then decreased until around day 0 values. This coincided with significant increased values of the antioxidants α-tocopherol and β-carotene in low salinity treatments over the control. These results suggest the existence of protection mechanisms against lipid peroxidation, and lead to the conclusion that the response to stress is species-specific, so that at the community level a change in the relative abundance of phytoplankton taxa appears as a response to hypoosmotic conditions. This could have important consequences for the trophic food web dynamics in areas influenced by high fresh water inputs.

1. Introduction

Phytoplankton are currently responsible for about 50% of global planetary primary production (Falkowski and Raven, 2007) and their change contributes as a substantial sink for CO_2 in marine ecosystems. Size structure is an important characteristic of phytoplankton communities, and relates to the magnitude of carbon fixed and exported into the deep sea (Armstrong et al., 2002; Schloss et al., 2007), as well as to the transfer of carbon to higher trophic levels (Waite et al., 1997). At the cellular level, phytoplankton size relates to physiological features such as growth, photosynthesis, respiration rates, light absorption (Finkel, 2001), as well as nutrient uptake and requirements (Hein et al., 1995).

Mean air temperatures along the Western Antarctic Peninsula have increased significantly (1–2 °C) over the past 50 years (Steig et al., 2009). This has long-term consequences on sea ice and ice shelf dynamics (Smith and Stammerjohn, 2001), as well as on glacial melting (Dierssen et al., 2002). Melting ice masses contribute to the globally rising sea level (Vaughan, 2006), promoting water column stratification, especially in shallow coastal environments, where freshwater is likely impacting on the structure and function of coastal food webs (Dierssen et al., 2002). In particular, Moline et al. (2004) have demonstrated an association between decreased salinities attributed to warmer environmental conditions and the dominance of cryptophytes rather than diatoms during austral summer. However, under low field surface salinity conditions in the Western Antarctic Peninsula Piquet et al. (2011) found changes to diatoms dominating the assemblages as well as in bacteria. Much of our current understanding on the effects of low salinity on marine phytoplankton is based on cultured algae under

* Corresponding author. Tel.: +54 11 6772 7574.
E-mail address: mhernando@cnea.gov.ar (M. Hernando).

http://dx.doi.org/10.1016/j.jembe.2015.02.012
0022-0981/

laboratory conditions (Fujii et al., 1999; Thessen et al., 2005; Petrou et al., 2011) and on limited observations from field studies (Vernet et al., 2011; Knox, 2007). To our knowledge, no experimental results are available on the response of Antarctic natural marine phytoplankton assemblages to changes in salinity. The variation in phytoplankton composition along salinity gradients has generally been ascribed to the fact that most phytoplankton species are stenohaline (i.e., having very narrow salinity tolerance range) and suffer osmotic stress upon exposure to salinity changes (Bisson and Kirst, 1995; Lionard et al., 2005). Any drastic change in salinity that is strong enough, could change local phytoplankton assemblages and establish a new stable community (Chakraborty et al., 2011). Low salinity stress in algae as well as in other plants severely disturbs the cellular homeostasis brought about by differences between the internal and exogenous concentration of inorganic ions (predominantly Na^+ and Cl^-), causing water influx, i.e., an increase in cell volume and ion efflux (Guillard, 1962). Thus, salt stress has effects on a variety of metabolic pathways, ranging from photosynthesis (Allakhverdiev et al., 2002), membrane lipid biosynthesis (Sakamoto and Murata, 2002; Singh et al., 2002), to an increase in cells' respiratory activity to maintain osmotic balance (Qasim et al., 1972). Some of the effects are mediated by the liberation of reactive oxygen species (ROS), causing additional oxidative stress (Mittler, 2002). Due to the inherent instability and reactivity of most ROS and their very low steady-state levels, their analysis is a much more difficult task than the determination of concentration of antioxidants and activities of antioxidant enzymes (Jakubowski and Bartosz, 2000). Oxidative stress has been linked to a number of cellular toxic processes, including damages to proteins (Prasad et al., 1995), membrane lipid peroxidation, enzyme inactivation and DNA breakage (Halliwell and Gutteridge, 2007). The membrane-permeable non-fluorescent 2-7-dichlorodihydrofluorescein diacetate (DCFH-DA) oxidation has been used for detecting several ROS in biological media (McDowell et al., 2013). DCFH-DA was initially thought to be useful as a specific indicator for hydrogen peroxide. However, it was already demonstrated that DCFH is oxidized by other ROS, including superoxide anion radical, hydroxyl radical, peroxyl, alkoxyl, hydroperoxyl and peroxynitrite which are products of normal metabolism (Halliwell and Gutteridge, 2007). The increased DCFH-DA oxidation will be referred to as an index of oxidative stress. It has been shown that ROS are responsible for the degradation of chlorophyll a and the decrease in the activity of photosystem II (PSII) in phytoplankton photosynthetic antenna (Saison et al., 2010), and cause inhibition of diatom growth (Hernando et al., 2011). However, it was also described that ROS might act as secondary messengers in the activation of stress-response signal transduction pathways and defence mechanisms (Mittler, 2002).

Diatoms present high activities of antioxidant enzymes, such as catalase, glutathione peroxidase and glutathione reductase and of non-enzymatic antioxidants such as the lipophilic alpha-tocopherol (αT), and beta-carotene (βC) allowing the cells to cope with potentially damaging conditions (Rijstenbil, 2001; Hernando et al., 2011).

Within this context, the main goal of the present study was to experimentally characterize the responses of a natural phytoplankton assemblage from a coastal Antarctic environment that is increasingly subject to changes in salinity by seasonal and long-term influx of freshwater from glacier melting (Rückamp et al., 2011). To reach this goal, we studied the phytoplankton assemblage's biomass, composition, growth and physiology (photosynthesis, respiration and oxidative stress). We hypothesize that low salinity stress induces significant changes in these parameters.

2. Materials and methods

2.1. Experimental set-up

The experiments were performed at Potter Cove (King George Island/25 de mayo, South Shetland Islands, Antarctica, 62°14′S, 58°38′W) in the Carlini (former Jubany) station facility from February 25th (Day 0) to March 5th 2011 (Day 8) using a natural plankton assemblage (Fig. 1). Before the experiment (on February 24th), six 100 l polyethylene tanks (microcosms) were thoroughly cleaned with diluted HCl and rinsed with distilled water. Seawater was collected at ~5 m depth in the outer Potter Cove (Fig. 1). The water was filtered through a 300 μm Nitex net placed inside a water distributor to avoid the passage of mesozooplankton and larger organisms. No nutrients were added to the water. Each microcosm was covered with plastic sheets between 23 h and 7 h of the following day and during storms in order to avoid contamination by particles, snow or fresh water from rain. Temperature and salinity were measured every 8 h using a Horiba U-10 conductimeter (Kyoto, Japan). Temperature was kept around 1 ± 0.7 °C, during the whole experiment, similar to the average in situ water temperature at the moment of sampling. To attain this, the microcosms were placed within a larger water tank connected to a stainless steel sea-water pump (Lowara, Italy), pumping coastal water from 4 to 6 m depth (varying with the tides) and ~25 m from the coastline. The water in each microcosm was mixed manually in order to maintain homogeneity in the water column and preventing cells from settling. The effectiveness of such procedure was previously confirmed (Hernando, 2011). The experimental design included two different salinity treatments (three replicates per treatment): a control with natural ambient salinity (34; Normal Salinity Treatment, NST), and low salinity conditions (30; Low Salinity Treatment, LST). The low value was chosen according to the average measurements, taken before the experiment, from the upper 5 m of Potter Cove in an area close to the Fourcade glacier during high fresh water run-off. In order to lower the salinity in the microcosms, 10 l of distilled water was added to each LST replicate. The same volume of GF/F filtered sea water was added to each replicate in NST, in order to keep the same dilution factor than for LST.

200 ml of water samples from each microcosm was taken at the beginning of the experiment and at days 1, 2, 4, 6 and 8 at 9 a.m. and filtered upon GF/F filters as follows: determination of chlorophyll-a (Chl a) content, DCFH-DA (Molecular Probes Inc, Eugene, OR, USA) oxidation rate, 2-thiobarbituric acid reactive substances (TBARS) content, αT and βC content assays. In addition, 150 ml were taken for cell counts. All these samples, except those taken for assessing DCFH-DA oxidation rate, which were analyzed few minutes after sampling, were stored during two months at −80 °C until analyses.

2.2. Chl a analyses and cell counts

Chl a filtrates were extracted in 7 ml absolute methanol (Holm-Hansen and Riemann, 1978). Fluorescence readings of the extracts (24 h later) were used for the calculation of Chl a concentration, after correction for phaeopigments (Holm-Hansen et al., 1965) and calibration with standard Chl a with a Shimadzu RF-1501 spectrofluorometer. Subsamples for the identification and enumeration of phytoplankton were fixed with an acidic lugol solution and kept it in cold, dark conditions until their analysis. In addition, qualitative phytoplankton samples were taken at the beginning and at the end of the experiment, concentrating the cells using a 20 μm mesh net. For quantitative estimations, cells were enumerated with a phase contrast Leica DMIL LED inverted microscope according to the procedures described by Utermöhl (1958). Subsamples were settled in a composite sedimentation chamber. At least 100 cells of the dominant taxa were counted in one or more strips of the chamber or random fields at 250 or 400×, depending on their concentration and size. The whole chamber bottom was also scanned at 100× to count large and sparse species. Cell biovolumes were calculated by approximation to the nearest geometric shapes proposed by Hillebrand et al. (1999). Cell carbon content was estimated with two different carbon-to-volume ratios, one for diatoms and one for all the other algae groups (Menden-Deuer and Lessard, 2000). Qualitative samples were examined using phase-contrast microscopy under a Leica DM 2500 microscope. For diatom frustules observation in order

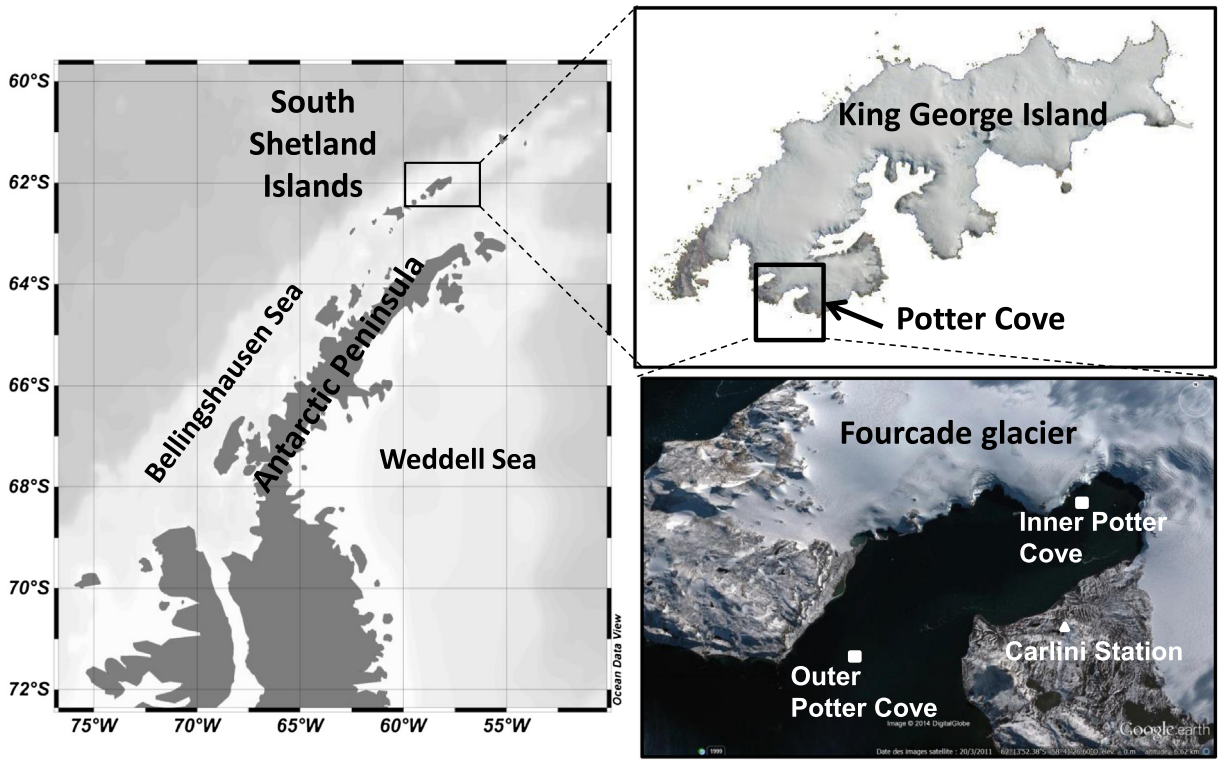

Fig. 1. Map showing the location of Potter Cove (62°14′S, 58°38′W) in King George/25 de mayo Island and the Antarctic Peninsula. White squares indicate both in situ sampling sites.

only to reveal the identity of the main species enumerated by inverted microscopy, organic material was removed from net subsamples using sodium hypochlorite as described in Almandoz et al. (2011). Clean material was then mounted in permanent slides using Naphrax® (The Biology Shop, Australia) following Ferrario et al. (1995). Further scanning electron microscopy observations were made with a Jeol JSM-6360 LV.

2.3. Growth measurements

Instantaneous growth rate (μ, ind^{-1}) was determined after the following equation:

$$\mu = \ln(N_i/N_{i-1})/(t_i - t_{i-1})$$

where t_i is the time of measurement and t_{i-1} is the previous day, N_i is the cell concentration at time t_i, and N_{i-1} is the cell concentration at the previous day.

2.4. Nutrient concentrations

Three replicate 50 ml samples were taken daily at 8 am from each microcosm for nutrients analyses (nitrate, phosphate and silicate). Samples were filtered onto precombusted Whatman GF/F filters, stored in acid-cleaned polypropylene bottles, and kept at −20 °C until analysis (within two months after the end of the experiment). Analyses were performed at the Centro Nacional Patagónico, Chubut, Argentina using an Auto Analyzer Technicon according to Treguer and Le Corre (1975), Eberlein and Kattner (1987) and Grasshoff et al. (1983).

2.5. DCFH-DA oxidation rate

Cellular generation of oxidants was determined by measuring the oxidation of DCFH-DA in vivo. DCFH-DA is a fluorogenic probe which passes through cell walls and membranes. During incubation, DCFH-DA is hydrolyzed, by intracellular hydrolytic deacetylation, to 2′, 7-dichlorofluorescin (DCFH) which is trapped inside the cell due to its polarity. This substance is then rapidly oxidized to the highly fluorescent compound 2′,7′-dichlorofluorescem (DCF) that allows the evaluation of cellular radical generation. According to the standard methods described by Bass et al. (1983), modified by Malanga et al. (2001), algae cells were incubated in the dark for 30 min in 2 ml of 40 mM Tris–HCl buffer (pH 7.0) in the presence of 5 μM DCFH-DA at 37 °C. Tris–HCl buffer (pH 7) is an appropriate medium for stabilizing several radical species and the used temperature assures the release of the oxidized dye to the incubation medium were fluorescence was assessed. The cells were removed after 30 min by centrifugation, and fluorescence in the supernatant (without cells) was monitored in a Shimadzu RF-1501 spectrofluorometer with excitation (λ_{ex}) at 498 nm and emission (λ_{em}) at 525 nm. In all cases, parallel blank controls with the reaction mixtures but laking the plankton community were included.

2.6. Content of TBARS

TBARS allow a rough estimate of the presence of aldehydes, yet most reactivity originates from malondialdehyde (MDA), a product of lipid peroxidation, wich can react with thiobarbituric acid under acidic and boiling conditions to allow a colorimetric assay (Janknegt et al., 2008). In consequence, cellular TBARS were used as an indicator of ROS-induced lipid peroxidation. The GF/F filters with cells were suspended in 2 ml of 120 mM KCl and 50 mM potassium phosphate buffer (pH 7.0), sonicated and centrifuged 10 min at 600 *g*. An aliquot (0.8 ml) of the supernatant was treated with 0.7 ml 30% (w/v) TCA and 50 mM potassium phosphate buffer (pH 7.0) and brought to a final volume of 2 ml before centrifugation. An aliquot of 0.2 ml of 3% (w/v) sodium dodecyl sulfate (SDS) and 0.05 ml of 4% (w/v) butylated hydroxytoluene (BHT) in ethanol were added to 1 ml of the supernatant. After mixing, 2 ml of 0.1 N HCl, 0.3 ml of 10% (w/v) phosphotungstic acid and 1 ml of 0.7% (w/v) 2-thiobarbituric acid were added. The mixture was heated at 95 °C in a water bath for 45 min and 5 ml of n-butanol were added and then the samples were vortexed and centrifuged at 600 *g* during 10 min. The fluorescence of the organic layer (upper layer) was measured at $\lambda_{ex} = 515$ nm and $\lambda_{em} = 555$ nm.

The values were expressed as nmol TBARS (malondialdehyde equivalents) per carbon units. Malondialdehyde standards were prepared from 1,1,3,3-tetramethoxypropane (Malanga and Puntarulo, 1995).

2.7. Content of lipid soluble antioxidants

The content of αT and βC in the sonicated cell homogenates were quantified filtering 5 ml samples by reverse-phase HPLC with electrochemical detection using a Bioanalytical Systems LC-4C amperometric detector with a glassy carbon working electrode at an applied oxidation potential of +0.6 V (Malanga and Puntarulo, 1995). Extraction from the samples was performed with 1 ml methanol and 4 ml hexane. After centrifugation at 600 *g* for 10 min, the hexane phase was removed and evaporated to dryness under N_2. Extracts were dissolved in methanol:ethanol (1:1 v/v) and injected for HPLC analysis. HPLC conditions were: isocratic reversed phase; column: Supelcosil LC-8; 3.3 cm × 4.6 cm × 3 μm; mobile phase: 20 mM lithium perclorate in methanol/water 99/1 (v/v), flow rate: 1 ml/min, retention time: αT = 0.8 min and βC = 1.6 min. D,L-αT from synthetic phytol (Sigma) and βC were used as standards.

2.8. Photosynthesis and respiration

Net oxygen production and respiration of the assemblages were measured according to Cole (1974). Water for these analyses was collected simultaneously with the rest of the samples. Dissolved oxygen concentrations were determined following the Modified Winkler Method (Labasque et al., 2004) using 250 ml BOD bottles, on a Pharmacia Ultrospec 3.000 photometer. Three-replicates for control (initial), clear and dark bottles were used for each of the treatments. The experimental bottles (i.e., the 3 clear and 3 dark) were suspended at 0.3 m depth in a water bath (opent-top, plastic tank) during 6–8 h around midday.

2.9. Statistical analyses

Repeated measurements ANOVA (RMANOVA) was performed (Statistica, version 9) to determine the significance of the differences observed in Chl a, DCFH-DA, TBARS, αT and βC concentrations as well as specific composition and abundance among treatments. Normality was verified using a one-sample Kolmogorov–Smirnov test, whereas the sphericity assumption that concerns variance homogeneity was checked using Mauchley's test. The main factors considered in the analysis were the number of days of exposure and the type of treatment. Tukey test was additionally performed to determine the differences between treatments. When interaction was significant or the assumptions of sphericity were not satisfied, a one factor ANOVA was performed evaluating the effect of treatment at different days of exposure (Scheiner, 2001). Arcsin transformation was applied in order to evaluate differences between percentages.

3. Results

3.1. Phytoplankton biomass and abundance

Chl a concentrations increased all along the experiment in NST, while a slight decrease until day 4 and a posterior increase until the end of the experiment were observed in LST. Here, concentrations were significantly lower than in NST for each day of the study ($p < 0.01$; Fig. 2A). Initial values were 5 ± 0.9 μg l^{-1} in both treatments. The maximum values reached during the study were 8 ± 2 μg l^{-1} and 35 ± 1 μg l^{-1} for LST and NST, respectively. Chl a and cell density showed a significant correlation for both treatments (not shown). In NST, the total cell number increased from day 1 up to the end of the experiment from an average of (44 ± 0.06) × 10^4 to (530 ± 1) × 10^4 cell l^{-1}, respectively. In contrast, in LST a significant increase was only observed from day 6 on, reaching (319 ± 19) × 10^4 cells l^{-1} at day 8

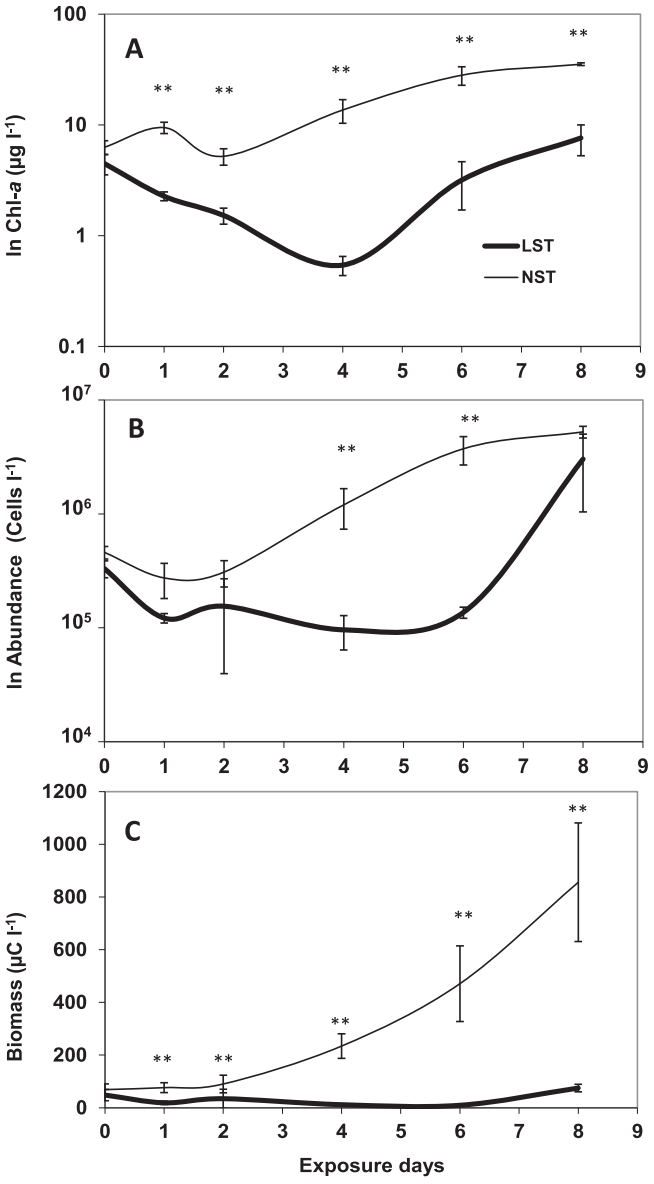

Fig. 2. Temporal evolution of (A) Ln Chl a (μg l^{-1}), (B) Ln Total phytoplankton assemblage (Cells l^{-1}) and (C) carbon biomass (μgC l^{-1}) of total diatom groups. Each point represents the mean ± SD. Significant (Tukey Test) differences between treatments at the same day are denoted with an * for $p < 0.05$ and ** for $p < 0.01$.

(Fig. 2B). RMANOVA analyses for total phytoplankton abundance (cells l^{-1}) showed a significant interaction between treatments and exposure time ($p < 0.05$). Significantly lower cell numbers were evident in LST compared to NST only on days 4 ((9 ± 2) × 10^4 and (120 ± 40) × 10^4 cells l^{-1} respectively; $p < 0.05$) and 6 ((140 ± 1) × 10^4 and (400 ± 1) × 10^4 cells l^{-1} respectively; $p < 0.01$). Total diatoms abundance showed a similar pattern to that described for total phytoplankton (Table 1). Estimated total phytoplankton carbon biomass was significantly higher in NST during all the experiment, with maximum values at day 8 (857 ± 207 μg C l^{-1}) compared with LST (76 ± 14 μg C l^{-1}) ($p < 0.01$) (Fig. 2C).

3.2. Phytoplankton composition

The main phytoplankton groups in the microcosms' assemblages were diatoms, cryptophytes, dinoflagellates, prasinophytes, silicoflagellates and other small unidentified phytoflagellates. Diatoms were the most abundant organisms, accounting on average

Table 1
Average ± standard deviation of cell density ($\times 10^4$ cell l^{-1}) of phytoflagellates, large centric and small pennate diatoms observed at experimental days. The asterisks indicate the degree of significance (** $p < 0.01$ and * $p < 0.05$) comparing density between treatments.

Treatment			Phytoflagellate < 5 μm			
	Day 0	Day 1	Day 2	Day 4	Day 6	Day 8
NST	(21 ± 0.7)	(6 ± 1)	(4 ± 2)	(10 ± 3)	(13 ± 9)	(29 ± 12)
LST	(19 ± 0.3)	(6 ± 2)	(4 ± 2)	(5 ± 4)	(7 ± 4)	(16 ± 5)
			Large Centric Diatoms			
NST	(17 ± 2)	(16 ± 6)**	(25 ± 9)*	(94 ± 11)**	(250 ± 51)**	(400 ± 7)**
LST	(14 ± 1)	(4 ± 1)	(10 ± 8)	(3 ± 1)	(7 ± 1)	(3 ± 2)
			Small Pennate Diatoms			
NST	(4 ± 3)	(0.8 ± 0.2)*	(0.7 ± 0.4)*	(14 ± 9)**	(98 ± 8)**	(100 ± 5)**
LST	(0.6 ± 0.3)	(0.5 ± 0.2)	(0.3 ± 0.2)	(0.6 ± 0.5)	(8 ± 5)	(280 ± 20)

for 46 (day 0) to 94% (day 8) of total phytoplankton cells along the experiment, and representing more than 90% of total carbon biomass along the study. In fact, the evolution of diatoms' abundance showed a similar pattern to that of Chl a, total phytoplankton abundance and carbon biomass (not shown). Relatively large centric diatom species, including *Odontella weissflogii*, *Porosira glacialis* and chains of *Thalassiosira antarctica*, *Chaetoceros tortissimus* and *C. socialis* dominated the assemblages in both treatments during the first two days of the experiment. From day 4 up to day 8, the specific composition observed in both treatments diverged. The abundance of large centric diatoms continued increasing in the NST, reaching 78% of total diatoms at day 8 (Fig. 3A, Table 1). By contrast, their abundance decreased in the LST and they were further replaced by small pennate diatoms mainly represented by *Navicula glaciei*, *N. perminuta*, *Nitzschia* cf. *lecointei* and *Fragilariopsis cylindrus/nana*. Significant differences in the relative abundance of large centric and small pennate diatoms (%) between NST and LST treatments were observed at days 6 and 8 ($p < 0.01$) (Fig. 3A). In synthesis, in LST the relative abundance of large centric diatoms at the beginning of the exponential phase was ~ 75% and the small pennate diatoms represented 25% of total diatoms. This changed to relative abundances of 1 and 99%, for large and small diatoms respectively on day 8. In contrast, no differences in the relative abundance of phytoplankton groups were found between the beginning and the end of the experiment in NST. In terms of carbon biomass, total diatoms increased around 13 times at the end of the experiment in NST, varying from (60 ± 20) μC l^{-1} at the beginning to (800 ± 200) μC l^{-1} at the last exposure day ($p < 0.01$). Contrastingly, there was only a small increase in carbon biomass of total diatoms at the end of the experiment in LST (60 ± 20 μC l^{-1} vs 75 ± 14 μC l^{-1}, beginning and end of experiment respectively, $p = 0.23$). Small pennate diatoms accounted for ~ 95% of total carbon biomass at the end of the experiments in LST but represented only 6% in NST (Fig. 3B). Their absolute value in terms of carbon biomass was significantly higher in LST compared with NST the end of the experiment (71 ± 15 μC l^{-1} vs 37 ± 21 μC l^{-1} for LST and NST respectively, $p < 0.05$). Finally, the abundance of phytoflagellates < 5 μm did not change between the beginning and the end of the experiment ($p = 0.89$, Table 1).

3.3. Phytoplankton growth rate

A decrease in phytoplankton assemblages' instantaneous growth rates (day^{-1}) was observed in both treatments during the first 24 h (adaptation period). Subsequently, in NST instantaneous growth rates increased continuously until day 4 (maximum average growth rate: 1.5 ± 0.6 d^{-1}), then gradually declined until the end of the experiment (average growth rate: 0.3 ± 0.2 d^{-1}) (Fig. 4). In LST, the instantaneous growth rates were significantly lower than in NST on day 4 (−0.5 ± 0.3 d^{-1} and 0.8 ± 0.3 d^{-1}, respectively) ($p < 0.05$) and day 6 (0.3 ± 0.2 d^{-1} and 1.3 ± 0.1, respectively) ($p < 0.01$). However, from day 4 on, growth rates increased exponentially until day 8, reaching significantly higher values in LST than in NST (3.0 ± 0.5 d^{-1} and 0.5 ± 0.2 d^{-1}, for days 6 and 8 respectively) ($p < 0.01$) (Fig. 4). RMANOVA showed a significant interaction between treatments and exposure time.

3.4. Nutrients

Initial nutrients' concentrations in both treatments averaged 11 ± 4, 1.3 ± 0.2 and 48 ± 3 μM for nitrate phosphate and silicate

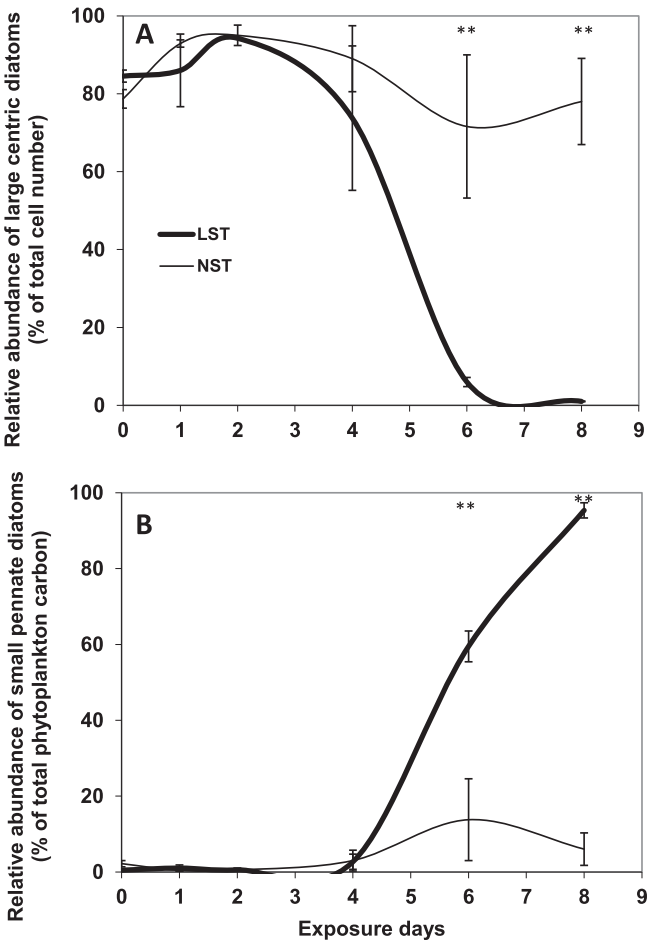

Fig. 3. Temporal evolution of (A) Relative abundance (%) of large diatoms (number of large in relation to total diatoms) under LST (30) or NST (34), (B) relative carbon biomass (%) of small pennate diatom when exposed to LST (30) or NST (34) treatments. Each point represents the mean ± SD. Significant (Tukey Test) differences between treatments at the same day are denoted with an * for $p < 0.05$ and ** for $p < 0.01$.

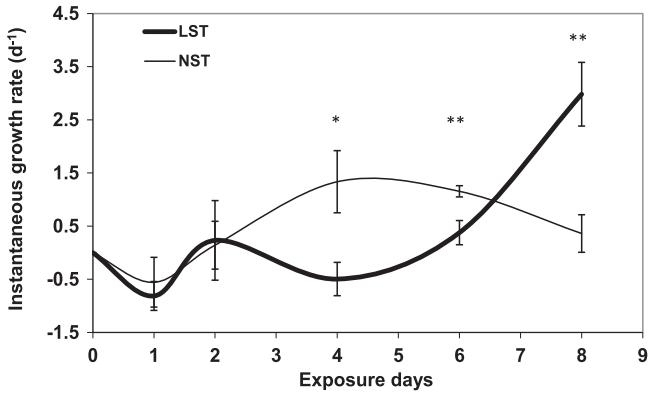

Fig. 4. Instantaneous growth rate of total phytoplankton using cell number, when exposed to LST (30) or NST (34). Each point represents the mean ± SD. Significant (Tukey Test) differences between treatments at the same day are denoted with an * for $p < 0.05$ and ** for $p < 0.01$.

concentrations, respectively (Fig. 5A, B and C). After day 2, and along with the observed increase in Chl a in the NST treatment, all studied nutrients showed a regular decreasing trend reaching minimal average concentrations on day 8 (5 ± 2, 0.64 ± 0.05 and 30 ± 5 μM for nitrate, phosphate and silicate, respectively). Moreover in LST on day 6, nitrate values increased and were significantly higher than values on days 0, 4 and 8 ($p < 0.01$) but lower than those on day 1 ($p < 0.01$). No significant differences were evident between exposure days 0, 1 and 2 in phosphate concentrations ($p = 0.2$). However, on days 4, 6 and 8 for NST, phosphate was significantly lower as compared to previous days and compared to LST ($p < 0.01$). In the case of silicate, the same trend was observed although no significant differences were found between treatments ($p = 0.14$) (Fig. 5 A, B and C).

3.5. DCFH-DA oxidation and presence of TBARS

Evidences of both reactive oxidant substances as well as of damage on cell membranes showed higher values in LST than in NST, except on day 8. DCFH-DA oxidation rates in LST were higher than in NST on day 1 ($p < 0.01$, Fig. 6A), and showed a significant increase on days 4 and 6 ($p < 0.05$). In contrast, TBARS content increased until day 2 and showed higher values in LST on days 4 and 6 ($p < 0.01$). Finally, no significant differences were found between treatments on day 8 neither for DCFH-DA oxidation nor for TBARS content ($p = 0.46$ and 0.36, respectively) (Fig. 6A, B). In LST, maximum values for both DCFH-DA oxidation and TBARS content were reached on days 6 and 2, respectively. On the other hand, in assemblages exposed to NST their concentrations were significantly higher on day 2 than during the rest of exposure days ($p < 0.01$, Fig. 6A, B).

3.6. Lipid soluble antioxidants

The content of the antioxidants αT and βC showed similar trends under both NST and LST (Fig. 7A, B). Cellular content of αT in LST was higher than in NST already on day 1 ($p < 0.05$), rising sharply and reaching maximum values of around 1 μmol cell^{-1} on day 4, which was also significantly higher than in NST samples ($p < 0.01$). A significant decrease was observed afterwards in both treatments until the end of the experiment. Despite this, the cell content of αT on day 6 was significantly higher in LST than in NST ($p < 0.01$). At the end of the experiment, the cell content of αT did not differ among treatments ($p = 0.79$), being significantly lower than the values measured on day 6 (Fig. 7A). The same trend was observed for the content of βC, but in this case concentrations were lower than those reported for αT (maximum concentration around 0.01 μmol cell^{-1} on days 1 and 2). Like αT, the

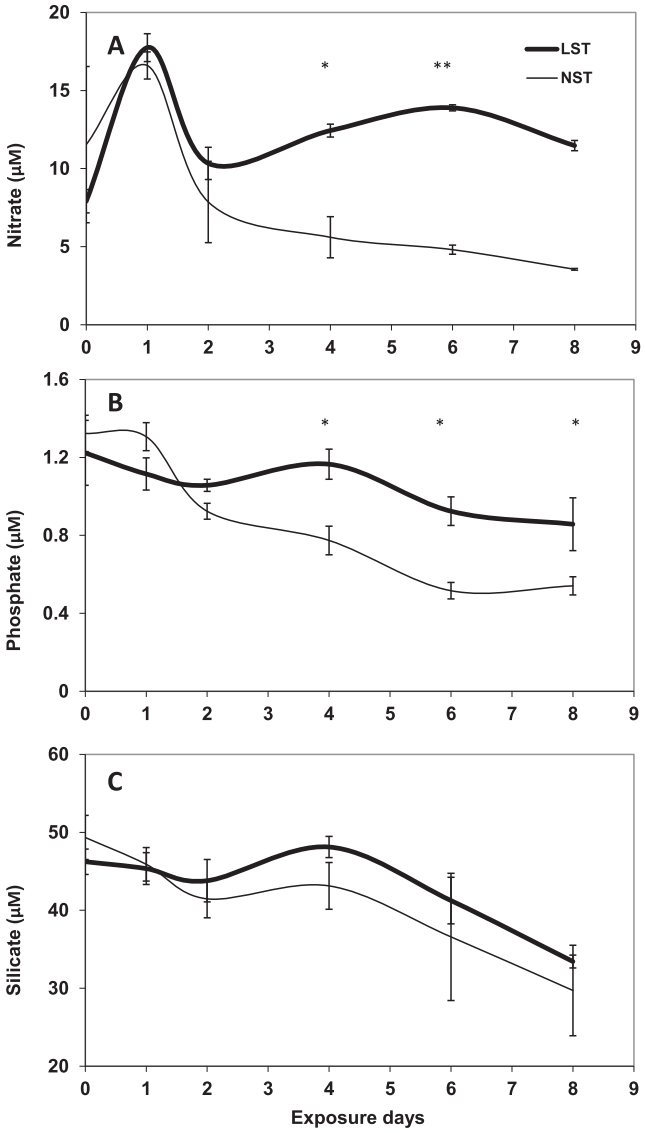

Fig. 5. Nutrients concentration in the experiments exposed to low and normal salinities. (A) nitrate (μM), (B) nitrite (μM), (C) orto-phosphate (μM), (D) silicate (μM). Each point represents the mean +/− SD. Significant (Tukey Test) differences between treatments at the same day are denoted with an * for $p < 0.05$ and ** for $p < 0.01$.

content of βC increased in LST on days 1 and 2 but did not show any significant differences between treatments or even with initial day concentrations ($p = 0.30$ and $p = 0.12$, respectively). Afterwards, significantly higher concentrations were found in LST than in NST on days 6 and 8 ($p < 0.01$ and $p < 0.05$, respectively) although concentrations were significantly lower ($p < 0.05$) on day 8 than on day 6 (Fig. 7B). The ratio βC:Chl a was significantly higher in LST than in NST ($p < 0.01$) for days 2, 6 and 8 (3, 7 and 9 fold increase, respectively). In addition, this index was significantly lower in the NST during days 6 and 8 as compared to days 0, 1 and 2 ($p < 0.01$). No significant differences in the βC:Chl a ratio were found among treatments on days 0 and 1 ($p = 0.25$ and 0.33, respectively).

3.7. Net community production and respiration

Net community production was significantly lower in LST than in NST on days 1, 2, 4 and 6 ($p < 0.01$, $p < 0.001$, $p < 0.001$ and $p < 0.05$, respectively). By contrast, no significant differences were found between treatments during the last day of the experiment ($p = 0.12$) (Fig. 8A).

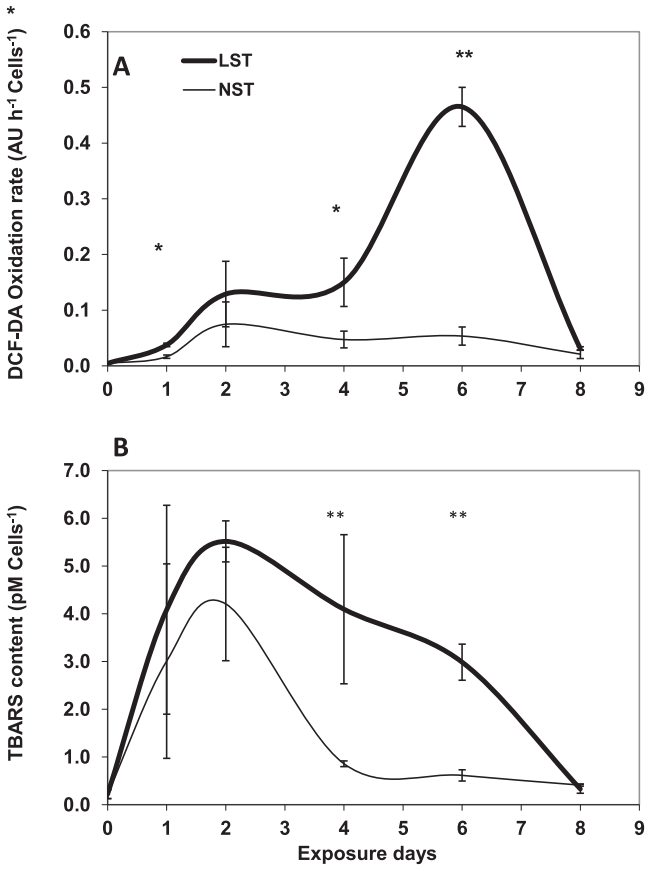

Fig. 6. Effect of salinity on oxidative stress parameters in plankton community as a function of exposure time. (A) DCFH-DA oxidation rate (expressed as arbitrary units in 1 h exposure), (B) lipid peroxidation (TBARS cell content). Each point represents the mean +/− SD. Significant (Tukey Test) differences between treatments at the same day are denoted with an * for $p < 0.05$ and ** for $p < 0.01$.

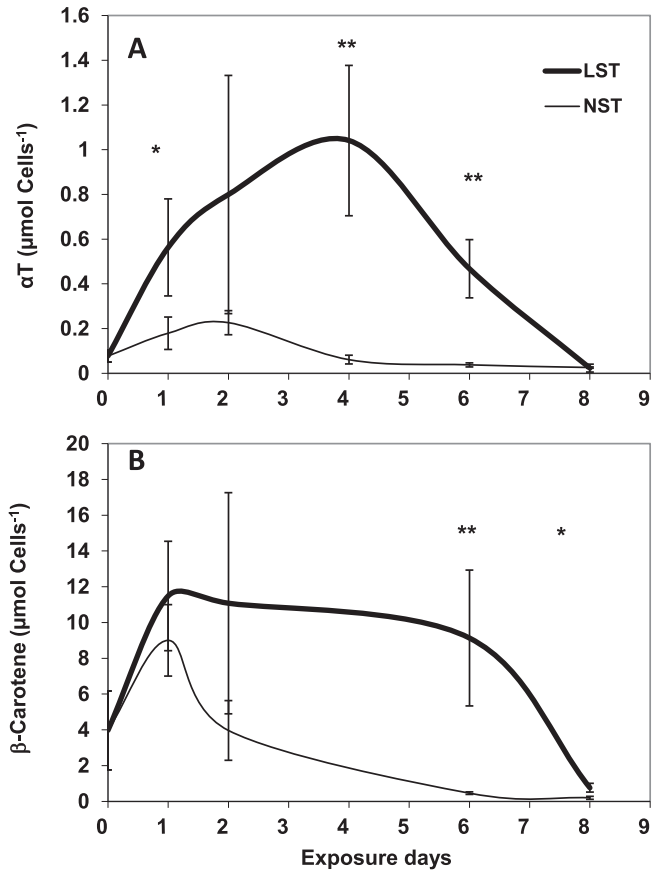

Fig. 7. Effect of salinity on lipid soluble antioxidants content: A) αT, B) βC, as a function of exposure time. Each point represents the mean ± SD. Significant (Tukey Test) differences between treatments at the same day are denoted with an * for $p < 0.05$ and ** for $p < 0.01$.

Respiration rates were significantly higher in LST than in NST during days 1, 2 and 4 ($p < 0.05$, $p < 0.01$ and $p < 0.01$, respectively). However, during days 6 and 8 no significant differences between treatments were evident ($p = 0.13$ and 0.95, respectively) (Fig. 8B).

4. Discussion

4.1. Changes in biomass and assemblages' composition

In this study, the relative decrease of phytoplankton biomass (both in terms of Chl a and phytoplankton carbon) and the change in phytoplankton assemblages' composition in LST are important effects of salinity diminution on marine plankton. The replacement of big centric diatoms by small pennate ones in LST meant a reduction of 91% in the amount of total phytoplankton carbon after 8 days of exposure. This evidences that the response to salinity fluctuations is species-specific (Karaeva and Jafarova, 1993; Aizdaicher and Markina, 2010; Piquet et al., 2011). Differential tolerance to osmotic stress is probably at the base of these observations. In some species, osmotic stress can modify transcription factors, leading to the expression of early response transcriptional activators, which then activate downstream stress tolerance effectors genes (Zhu, 2002). For example, in *F. cylindrus* (one of the small pennate diatom that increased in relative abundance at the end of the experiment in LST) specific fractions of sequences were found that might harbour genes necessary for adaptation to extreme environmental conditions in polar oceans and sea ice (Mock et al., 2006). Field studies on the distribution patterns of specific Antarctic diatoms also showed the prevalence of the observed small species under low salinity conditions. For example, although *Fragilariopsis* sp. is frequently observed in pelagic environments (Kopczynska et al., 2007), it is particularly abundant in older sea ice floes (Lizotte, 2001) and is also found in high numbers in meltwater (Beans et al., 2008).

The decrease in salinity caused morphological changes (observed microscopically) in big diatoms: cell size increased, chloroplasts were compressed, protoplasm became granular and cytoplasm retracted. The irreparable destruction of big diatoms' cells due to hydration, as a result of hypotonic stress may be one of the reasons of their overall decay. Furthermore, our experimental results could be probably extrapolated to the environment. During 2010 in Potter Cove, a large microphytoplankton bloom dominated by centric diatoms (i.e. *Porosira glacialis*, *Thalassiosira antarctica* and *T. ritscheri*) did not survive after a significant increase in meltwater that led to surface salinities values < 32 (Hernando et al., unpublished results). After this, the pennate diatom *Pseudogomphonema kamtschaticum* increased in relative abundance, and one month later, towards the end of February, diatoms had been replaced by small crytophytes. It had been hypothesized that a differential sensitivity of microplanktonic diatoms to low salinity was a possible cause of this change (Schloss et al., 2014), which can now be confirmed with the present results. Our results are consistent with those of Li et al. (2009), who found that small phytoplankton cells increased while larger ones decreased under meltwater conditions and episodic input of large river runoff in the Arctic Ocean.

4.2. Phytoplankton physiological responses

Osmotic stress has been shown to inhibit phytoplankton growth rates (Aizdaicher and Markina, 2010). Diminution of instantaneous growth rates observed in LST was probably related to the large centric diatoms' decay (see above), that resulted from a negative balance

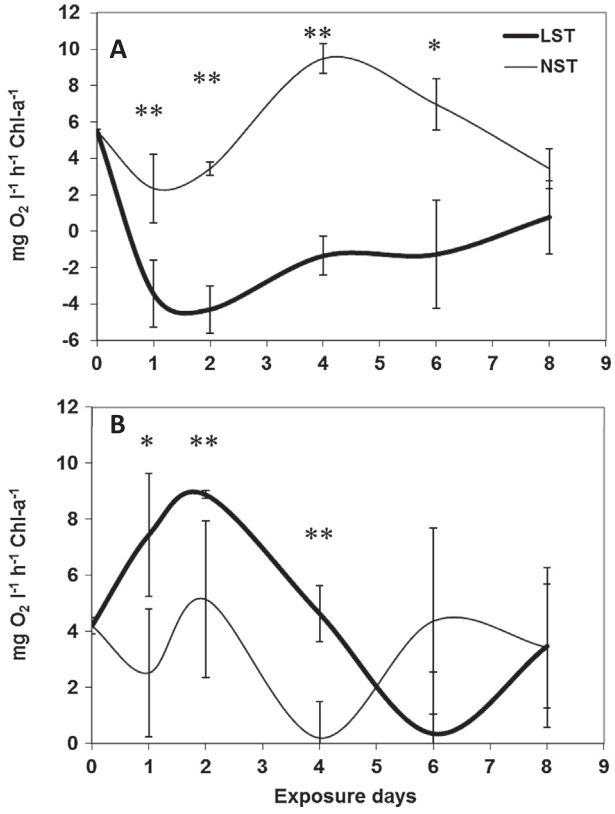

Fig. 8. (A) Hourly rates of net primary production, (B) Hourly rates of oxygen consumption. Each point represents the mean +/− SD. Significant (Tukey Test) differences between treatments at the same day are denoted with an * for $p < 0.05$ and ** for $p < 0.01$.

between osmotic stress and protection mechanisms. When this group was later replaced by small pennate diatoms in LST, by the end of the experiment, phytoplankton assemblages' growth rate (estimated on cell numbers) was significantly higher in LST than in NST. Changes in salinity can strongly influence Antarctic phytoplankton photosynthesis (Palmisano et al., 1987; Ralph et al., 2005, 2007). Salt stress has been shown to suppress not only the de novo synthesis of the D1 protein but also the synthesis of almost all other proteins at both the transcriptional and the translational levels (Allakhverdiev et al., 2002). The significant decrease in net photosynthesis in our LST microcosms could be due to a decreased efficiency of absorbed light energy utilization by PSII under hipoosmotic conditions, as shown by Radchenko and Il´yash (2006). These authors also described species-specific responses to hypotonic stress of different severity and the possible presence of species-specific mechanisms of osmotic acclimation. Primary inhibition of photosynthetic activity by hypotonic stress is commonly followed by full or partial restoration of photosynthetic parameters. The time required for recovery differs between individual algal species and depends on the degree of such type of stress (Radchenko and Il´yash, 2006). One of the species dominating the phytoplankton assemblage at day 8 in LST, *Fragilariopsis cylindrus/nana* presents a relatively constant photosynthesis response in environments submitted to variable salinity (Petrou et al., 2011), which contributes to explain the good adaptation of this species to the low saline conditions of our treatments.

Respiration rates in plankton exposed to low salinity conditions showed significantly higher values over control only during days 1, 2 and 4. It should be noted that overall microzooplankton only represented a small fraction of total phytoplankton abundance (0.7%) at the beginning of the experiment, and that a diminishing trend in their abundance was observed in both treatments, with no differences among them (0.01%, $p = 0.36$) (data not shown). Therefore, the higher respiration rates in LST samples, was probably not related to microzooplankton respiration.

An early increase in phytoplankton respiration was probably needed to deal with the stress induced by low salinity. ROS are generated by the conversion of normal by-products of cell respiration, such as hydrogen peroxide and the superoxide anion, into highly damaging radical species. The increase in respiration that we observed in LST may be in addition partially due to bacterial respiration, which we did not measure. Bacterial production is generally assumed to be equivalent to about 25–30% of phytoplankton primary production rates, based on estimations from a wide range of marine Antarctic ecosystems (Ducklow et al., 2000). Likewise, Morán et al. (2006) measured the activity of heterotrophic bacterioplankton, determined by [^{3}H] leucine incorporation, in eight stations located in the vicinity of the Antarctic Peninsula (62–66°S) and confirmed the low activities found in previous studies, which contrasts with findings from lower latitudes (Morán et al., 2001; Oliver et al., 2004). Therefore, we assume that bacterial respiration was both low and similar in all treatments and that the significant differences in community respiration among treatments observed during days 1, 2 and 4 are mainly due to phytoplankton metabolism.

It is worth mentioning that during summer 2010 the response of Potter Cove phytoplankton assemblages to natural variations in salinity was similar to what we observed in our microcosms (Hernando et al., unpublished data; mentioned above). During an episode of intense glacier melting, phytoplankton from inner Potter Cove, presented DCFH-DA oxidation rates and respiration values significantly higher than those from an area far from glacier influence (0.62 *vs* 0.3 UA h^{-1}, and 100 *vs* 60 mg O_2 l^{-1} h^{-1}, respectively; $p < 0.05$) (Fig. 1). In addition, significantly lower net phtosynthesis was observed near the glacier area than far from it (35 *vs* 15 mg O_2 l^{-1} h^{-1}, respectively; $p < 0.05$).

4.3. Balance between osmotic stress and protection at the cellular level

Osmotic stress is caused by a flux of water across the semi permeable cell membrane that leads to a change of the cellular water potential (Bisson and Kirst, 1995). One of the mechanisms to reduce the osmotic pressure in diatoms is the extracellular release of amino acids and glucose (Rijstenbil et al., 1989). The significant increase in nitrate concentration observed in LST after day 2 might be related to both the result of big diatoms lysis as well as the controlled release of specific substances such as aminoacids, to reduce intracellular turgor pressure (Radchenko and Il´yash, 2006). Big diatoms contain internal vacuoles for nutrient storage (Lomas and Glibert, 2000) that represent 30–90% of total cell volume (Smayda, 1970) and which could have released nigrogen-rich mollecules to the water.

Hypoosmotic conditions have been demonstrated to stimulate the generation of ROS (Petrou et al., 2011; Häubner et al., 2014). Intracellular production of ROS does not necessarily imply cellular toxicity, but oxidative stress will occur when ROS formation exceeds antioxidant defence capability or disrupts redox signalling, affecting cell functionality (Häubner et al., 2014). In our experiment, DCFH-DA oxidation increased until day 6 in LST, increasing 9-fold as compared to NST values. In addition, TBARS concentration, an indicator of lipid biological membranes peroxidation of unsaturated fatty acids, presented a trend similar to that of DCFH-DA oxidation, but maximum values were observed on day 2, after which the cellular concentrations decreased until the end of the experiment. This suggests that the effects of low salinity on cell membranes are likely related to oxidation by free radicals. For *T. weissflogii* it has been shown that a decreased abundance within the first day of exposure to a low salinity medium is related to the loss of membrane integrity, which did not allow a controlled release of specific substances to decrease intracellular turgor pressure (Radchenko and Il´yash, 2006).

Organisms have protective mechanisms against harmful stress, including a number of enzymatic and non-enzymatic defences that together constitute a complex antioxidant defence network (Häubner

et al., 2014). In the present study we observed a significant increase in αT concentrations in LST until day 4, in coincidence with a decrease in TBARS content. This suggests that after the generation of ROS during the first days of exposure to LST, ROS were compensated by means of the consumption of antioxidants. Lipophilic molecules, such as αT, are able to deactivate singlet oxygen ($^1O_2$), reduce O_2 and terminate lipid radical chain reactions (Häubner et al., 2014), and are regenerated by ascorbate. Hernando et al. (2011) showed that Antarctic diatoms are able to produce αT in response to other stress sources, such as the stress induced by UV radiation. In this sense, our present results on the protective role of αT against hypoosmotic-induced damage, especially in centric diatoms, are in coincidence with previous findings (Häubner et al., 2014). However, despite antioxidant protection, centric diatoms were not able to cope with the osmotic stress in LST. Microscopic analysis showed deformed cells and broken frustules in LST after day 4, possibly due to the destruction of their membranes.

Although βC content showed a similar trend than αT, on day 8 its concentration was significantly higher in LST than in NST. βC acts as both an antenna pigment in the photosynthesis process (Hernando et al., 2005; Häubner et al., 2014), and is (as zeaxanthin as well) a lipophilic antioxidant protecting cells against oxidative damage initiated by $^1O_2$ and also quenching $^1O_2$ preventing the formation of chlorophyll triplet excited state (Frank and Brudvig, 2004). Furthermore, βC is a major precursor for the carotenoids of the xanthophyll cycle in plants (Demmig-Adams and Adams, 2002). As a part of antioxidant mechanisms xanthophylls can increase their ratio in relation to light harvesting pigments (Harris et al., 2005; Van De Poll et al., 2005). In our experiment, values of βC:Chl a ratio were significantly higher in LST as compared to NST, suggesting that βC production provided an important antioxidant protection for small pennate diatoms. The low ROS (TBARS) content on day 8 might be due to a protection strategy exerted by lipid antioxidants. The dominance of small diatoms can be explained by the high cell βC concentration observed, and therefore, their capacity to avoid oxidative damage.

The link between physiological plasticity and longer-term ecological niche adaptation to meltwater displayed by small phytoplankton, which led to a change in size structure of the phytoplankton community, may have important consequences for the whole food web (Legendre and Rassoulzadegan, 1996) and affect the carbon cycling in the ocean (Finkel et al., 2010). The fact that large phytoplankton can sustain rates of production and biomass higher than those of small cells (Cermeño et al., 2005; Claustre et al., 2005; Marañón et al., 2007) has also biogeochemical implications, because larger cells are responsible for most of the export of biogenic carbon towards the deep ocean and upper trophic levels (Legendre and Rassoulzadegan, 1996).

Acknowledgments

We would especially like to thank Oscar González, from the Antarctic Institute of Argentina, for fieldwork and laboratory support at Carlini station, as well as to Alejandro Ulrich and Silvia Rodríguez. Our thanks also to the personnel from the Alfred-Wegener-Institut (AWI), who shared equipment and results with us in the frame of the Argentinean-German Cooperation at Carlini-Dallmann in Potter Cove, Antarctica. This study was supported by the National Agency for the Promotion of Science and Technology of Argentina (ANPCYT) (PICTO 2005-35562 and PICT 2011-1320) to Irene R. Schloss, the Antarctic Institute of Argentina and CONICET and PICT 2012-00845 and by the Universidad de Buenos Aires (UBACyT 20020100100555) and CONICET (PIP 11220110100697) to S. Puntarulo. This study is part of the Impact of climate induced glacial melting on marine coastal systems in the Western Antarctic Peninsula Region (IMCOAST, European Science FoundationPolar CLIMATE) supported by the European Polar Consortium and the IMCONet — Interdisciplinary Modelling of Climate Change in Coastal Western Antarctica — Network for Staff Exchange and Training, FP7-PEOPLE-2012-International Research Staff Exchange Scheme (IRSES) 318718. **[SS]**

References

Aizdaicher, N.A., Markina, Z.V., 2010. The effect of decrease in salinity on the dynamics of abundance and the cell size of *Corethron hystrix* (Bacillariophyta) in Laboratory Culture. Ocean Sci. J. 45, 1–5.

Allakhverdiev, S.I., Nishiyama, Y., Miyairi, S., Yamamoto, H., Inagaki, N., Kanesaki, Y., Murata, N., 2002. Salt stress inhibits the repair of photodamaged photosystem II by suppressing the transcription and translation of *psbA* genes in *Synechocystis*. Plant Physiol. 130, 1443–1453.

Almandoz, G.O., Hernando, M., Ferreyra, G., Schloss, I.R., Ferrario, M.E., 2011. Seasonal phytoplankton dynamics in extreme southern South America (Beagle Channel, Argentina). J. Sea Res. 66, 47–57.

Armstrong, R.A., Lee, C., Hedges, J.I., Honjo, S., Wakeham, S.G., 2002. A new mechanistic model for organic carbon fluxes in the ocean based on the quantitative association of POC with ballast minerals. Deep-Sea Res. II 49, 219–236.

Bass, D.A., Parce, J.W., Dechatelet, L.R., Szejda, P., Seeds, M.C., Tiomas, M., 1983. Flow cytometrie studies of oxidative product formation by neutrophils: a graded response to membrane stimulation. J. Immunol. 130, 1910–1917.

Beans, C., Hecq, J.H., Koubbi, P., Vallet, C., Wright, S., Goffart, A., 2008. A study of the diatom-dominated microplankton summer assemblages in coastal waters from Terre Adelie to the Mertz Glacier, East Antarctica (139E–145E). Polar Biol. 31, 1101–1117.

Bisson, M.A., Kirst, G.O., 1995. Osmotic acclimation and turgor pressure regulation in algae. Naturwissenschaften 82, 461–471.

Cermeño, P., Marañón, E., Rodríguez, J., Fernandéz, E., 2005. Large-sized phytoplankton sustain higher carbon-specific photosynthesis than smaller cells in a coastal eutrophic ecosystem. Mar. Ecol. Prog. Ser. 297, 51–60.

Chakraborty, P., Acharyya, T., Babu, P.R., Bandyopadhyay, D., 2011. Impact of salinity and pH on phytoplankton community in a tropical freshwater system: an investigation with pigment analysis by HPLC. J. Environ. Monit. 13, 614–620.

Claustre, H., Babin, M., Merien, D., Ras, J., Prieur, L., Dallot, S., 2005. Toward a taxon-specific parameterization of bio-optical models of primary production: a case study in the North Atlantic. J. Geophys. Res. 110, C07S12.

Cole, G.A., 1974. Textbook of Limnology. C. V. Mosby Company, Publishers, Saint Louis.

Demmig-Adams, B., Adams, W., 2002. Antioxidants in photosynthesis and human nutrition. Science 298, 2149–2153.

Dierssen, H.M., Smith, R.C., Vernet, M., 2002. Glacial meltwater dynamics in coastal waters West of the Antarctic Peninsula. Proc. Natl. Acad. Sci. U. S. A. 99, 1790–1795.

Ducklow, H., Dickson, M.L., Kirchman, D.L., Steward, G., Orchardo, J., Marra, J., Azam, F., 2000. Constraining bacterial production, conversion efficiency and respiration in the Ross Sea, Antarctica, January–February, 1997. Deep-Sea Res. II 47, 3227–3247.

Eberlein, K., Kattner, G., 1987. Automatic method for the determination of orthophosphate and total disolved phosphorous in the marine environment. Fresenius' Z. Anal. Chem. 326, 354–357.

Falkowski, P.G., Raven, J.A., 2007. Aquatic Photosynthesis. Princeton University Press, Princeton.

Ferrario, M.E., Sar, E.A., Sala, S., 1995. Metodología básica para el estudio del fitoplancton con espacial referencia a las diatomeas. In: Alveal, K., Ferrario, M.E., Oliveira, E.C., Sar, E.A. (Eds.), Manual de Métodos Ficológicos. Universidad de Concepción, Editora A. Pinto, Chile, pp. 1–23.

Finkel, Z.V., 2001. Light absorption and size scaling of light-limited metabolism in marine diatoms. Limnol. Oceanogr. 46, 86–94.

Finkel, Z.V., Beardall, J., Flynn, K.J., Quigg, A., Rees, T.A.V., Raven, J.A., 2010. Phytoplankton in a changing world: cell size and elemental stoichiometry. J. Plankton Res. 32, 119–137.

Frank, H., Brudvig, G., 2004. Redox functions of carotenoids in photosynthesis. Biochemistry 43, 8607–8615.

Fujii, S.R., Yamamoto, S., Nakayama, Y.S., Broady, P.A., 1999. Effects of salinity on growth and content of intracellular solutes in *Heterococcus* sp. (Tribonennatales, Xanthophyceae) from Antarctica. Phycol. Res. 47, 65–69.

Grasshoff, K., Ehrhardt, M., Kremling, K., Almgren, T., 1983. Methods of seawater analysis. Verlag Chemie, Weinheim, Germany, p. 419.

Guillard, R.R.L., 1962. Salt and osmotic balance. In: Lewin, R.A. (Ed.), Physiology and Biochemistry of Algae. Academic Press, New York and London.

Halliwell, B., Gutteridge, J.M., 2007. Free Radicals in Biology and Medicine. Oxford University Press, New York.

Harris, G.N., Scanlan, D.J., Geider, R.J., 2005. Acclimation of Emiliania huxleyi (Prymnesiophyceae) to photon flux density. J. Phycol. 41, 851–862.

Häubner, N., Sylvander, P., Vuori, K., Snoeijs, P., 2014. Abiotic stress modifies the synthesis of alpha-tocopherol and beta-carotene in phytoplankton species. J. Phycol. 50, 753–759.

Hein, M., Folager Pedersen, M., Sand-Jensen, K., 1995. Size-dependent nitrogen uptake in micro- and macroalgae. Mar. Ecol. Prog. Ser. 118, 247–253.

Hernando, M.P., 2011. Fitoplancton de altas latitudes en condiciones de ozono disminuido. Editorial Académica Española, p. 300. ISBN-10: 3846560545.

Hernando, M., Malanga, G., Ferreyra, G.A., 2005. Oxidative stress and antioxidant defences generated by solar UV in a Subantarctic marine phytoflagellate. Sci. Mar. 69, 287–295.

Hernando, M., Malanga, G., Puntarulo, S., Ferreyra, G., 2011. Non-enzymatic antioxidant photoprotection against potential UVBR-induced damage in an Antarctic diatom (*Thalassiosira* sp.). Lat. Am. J. Aquat. Res. 39, 397–408.

Hillebrand, H., Dürselen, C.D., Kirschtel, D., Pollingher, U., Zahorí, T., 1999. Biovolume calculation for pelagic and benthic microalgae. J. Phycol. 35, 403–424.

Holm-Hansen, O., Riemann, B., 1978. Chlorophyll a determination: improvements in methodology. Oikos 30, 438–447.
Holm-Hansen, O., Lorenzen, C.J., Holmes, R.W., Strickland, J.D., 1965. Fluorometric determination of chlorophyll. J. Cons. Int. Explor. Mer 30, 3–15.
Jakubowski, W., Bartosz, G., 2000. 2,7-Dichlorofluorescin oxidation and reactive oxygen species: what does it measure? Cell Biol. Int. 24, 757–760.
Janknegt, P.J., van de Poll, W.H., Visser, R.J.W., Rijstenbil, J.W., Buma, Anita G.J., 2008. Oxidative stress responses in the marine antarctic diatom *Chaetoceros brevis* (bacillariophyceae) during photoacclimation. J. Phycol. 44, 957–966.
Karaeva, N.I., Jafarova, S.K., 1993. Experimental investigations of euryhaline Bacillariophyta in relation to salinity variations. Algologia 3, 97–105.
Knox, G.A., 2007. Biology of the Southern Ocean. 2nd edition. CRC Press, Boca Raton, FL.
Kopczynska, E.E., Savoye, N., Dehairs, F., Cardinal, D., Elskens, A., 2007. Spring phytoplankton assemblages in the Southern Ocean between Australia and Antarctica. Polar Biol. 31, 77–88.
Labasque, T., Chaumery, C., Aminot, A., Kergo, G., 2004. Spectrophotometric Winkler determination of dissolved oxygen: re-examination of critical factors and reliability. Mar. Chem. 88, 53–60.
Legendre, L., Rassoulzadegan, F., 1996. Food-web mediated export of biogenic carbon in oceans. Mar. Ecol. Prog. Ser. 145, 179–193.
Li, W.K.W., Mc Laughlin, F.A., Lovejoy, C., Carmack, E.C., 2009. Smallest algae thrive as the Arctic Ocean freshens. Science 326, 539.
Lionard, M., Muylaert, K., Van Gansbeke, D., Vyverman, W., 2005. Influence of changes in salinity and light intensity on growth of phytoplankton communities from the Schelde river and estuary (Belgium/The Netherlands). Hydrobiologia 540, 105–115.
Lizotte, M.P., 2001. The contributions of sea ice algae to Antarctic Marine primary production. Am. Zool. 41, 57–73.
Lomas, M., Glibert, P., 2000. Comparison of nitrate uptake, storage and reduction in marine diatoms and flagellates. J. Phycol. 36, 903–913.
Malanga, G., Puntarulo, S., 1995. Oxidative stress and antioxidant content in *Chlorella vulgaris* after exposure to ultraviolet-B radiation. Physiol. Plant. 94, 672–679.
Malanga, G., Juarez, A.B., Albergheria, J.S., Veléz, C.G., Puntarulo, S., 2001. Efecto de la radiación UVB sobre el contenido de ascorbato y radical ascorbilo en algas verdes. In: Alveal, K., Antezana, T. (Eds.), Sustentabilidad de la Biodiversidad, un problema actual, bases científico-técnicas, teorizaciones y proyecciones. Concepción, Chile, pp. 389–398.
Marañón, E., Cermeño, P., Rodríguez, J., Zubkov, M.V., Harris, R.P., 2007. Scaling of phytoplankton photosynthesis and cell size in the ocean. Limnol. Oceanogr. 52, 2190–2198.
McDowell, R.E., Amsler, C.D., Dickinson, D.A., McClintock, J.B., Baker, B.J., 2013. Reactive oxygen species and the Antarctic macroalgal wound response. J. Phycol. 50, 71–80.
Menden-Deuer, S., Lessard, E.J., 2000. Carbon to volume relationships for dinoflagellates, diatoms, and other protist plankton. Limnol. Oceanogr. 45, 569–579.
Mittler, R., 2002. Oxidative stress, antioxidants, and stress tolerance. Trends Plant Sci. 7, 405–410.
Mock, T., Krell, A., Glockner, G., Kolukisaoglu, U., Valentin, K., 2006. Analysis of expressed sequence tags (ESTs) from the polar diatom *Fragilariopsis cylindrus*. J. Phycol. 42, 78–85.
Moline, M.A., Claustre, T., Frazer, O., Schofield, O., Vernet, M., 2004. Alteration of the food web along the Antarctic Peninsula in response to a regional warming trend. Global Change Biology 10 (12), 1973–1980.
Morán, X.A.G., Gasol, J.M., Pedrós-Alió, C., Estrada, M., 2001. Dissolved and particulate primary production and bacterial production in offshore Antarctic waters during austral summer: coupled or uncoupled? Mar. Ecol. Prog. Ser. 222, 25–39.
Morán, X.A.G., Sebastián, M., Pedrós-Alió, C., Estrada, M., 2006. Response of Southern Ocean phytoplankton and bacterioplankton production to short-term experimental warming. Limnol. Oceanogr. 51, 1791–1800.
Oliver, J.L., Barber, R.T., Smoth, W.O., Ducklow, H.W., 2004. The heterotrophic bacterial response during the Southern Ocean Iron Experiment (SOFeX). Limnol. Oceanogr. 49, 2129–2140.
Palmisano, A.C., Soohoo, J.B., Moe, R.L., Sullivan, C.W., 1987. Sea ice microbial communities. VII. Changes in under-ice spectral irradiance during the development of Antarctic sea ice microalgal communities. Mar. Ecol. Prog. Ser. 35, 165–173.
Petrou, K., Doblin, M.A., Ralph, P.J., 2011. Heterogeneity in the photoprotective capacity of three Antarctic diatoms during short-term changes in salinity and temperature. Mar. Biol. 158, 1029–1041.
Piquet, A., Henk Bolhuis, M.T., Meredith, M.P., Buma, A.G.J., 2011. Shifts in coastal Antarctic marine microbial communities during and after meltwater-related surface stratication. FEMS Microbiol. Ecol. 1, 1–15.
Prasad, T.K., Anderson, M.D., Stewart, C.R., 1995. Localization and characterization of peroxidases in the mitochondria of chilling acclimated maize seedlings. Plant Physiol. 108, 1597–1605.
Qasim, S.Z., Bhattathiri, P.M., Devassy, V.P., 1972. The influence of salinity on the rate of photosynthesis and abundance of some tropical phytoplankton. Mar. Biol. 12, 200–206.
Radchenko, I.G., Il´yash, L.V., 2006. Growth and photosynthetic activity of the diatom *Thalassiosira weissflogii* under low salinity conditions. Izv. RAN Ser. Biol. 3, 306–313.
Ralph, P.J., Mcminn, A., Ryan, K., Ashworth, C., 2005. Short-term effect of temperature on the photokinetics of microalgae from the surface layers of Antarctic pack ice. J. Phycol. 41, 763–769.
Ralph, P.J., Ryan, K.G., Martin, A., Fenton, G., 2007. Melting out of sea ice causes greater photosynthetic stress in algae than freezing in. J. Phycol. 43, 948–956.
Rijstenbil, J.W., 2001. Effects of periodic low UVA radiation on cell characteristics and oxidative stress in the marine planktonic diatom *Ditylum brightwellii*. Eur. J. Phycol. 36, 1–8.
Rijstenbil, J.W., Mur, L.R., Wijnholds, J.A., Sinke, J.J., 1989. Impact of a temporal salinity decrease on growth and nitrogen metabolism of the marine diatom *Skeletonema costatum* in continuous cultures. Mar. Biol. 101, 121–129.
Rückamp, M., Braun, M., Suckro, S., Blindow, N., 2011. Observed glacial changes on the King George Island ice cap, Antarctica, in the last decade. Glob. Planet. Chang. 79, 99–109.
Saison, C., Perreault, F., Daigle, J.C., Fortin, C., Claverie, J., Morin, M., Popovic, R., 2010. Effect of core–shell copper oxide nanoparticles on cell culture morphology and photosynthesis (photosystem II energy distribution) in the green alga, *Chlamydomonas reinhardtii*. Aquat. Toxicol. 96, 109–111.
Sakamoto, A., Murata, N., 2002. The role of glycine betaine in the protection of plants from stress: clues from transgenic plants. Plant Cell Environ. 25, 163–171.
Scheiner, S.M., 2001. MANOVA: multiple response variables and multispecies interactions. In: Scheiner, Gurevitch (Eds.), Design and Analysis of Ecological Experiments, 2nd ed. Oxford Univ. Press, Oxford.
Schloss, I.R., Ferreyra, G.A., Ferrario, M.E., Almandoz, G.O., Codina, R., Bianchi, A.A., Balestrini, C.F., Ochoa, H.A., Ruiz Pino, D., Poisson, A., 2007. Role of plankton communities in sea–air variations in pCO_2 in the SW Atlantic Ocean. Mar. Ecol. Prog. Ser. 332, 93–106.
Schloss, I.R., Wasilowska, A., Dumont, D., Almandoz, G.O., Hernando, M.P., Michaud-Tremblay, C.A., Saravia, M., Rzepecki, L., Monien, P., Monien, D., Kopczyńska, E.E., Bers, A.V., Ferreyra, G.A., 2014. On the phytoplankton bloom in coastal waters of southern King George Island (Antarctica) in January 2010: an exceptional feature? Limnol. Oceanogr. 59 (1), 195–210.
Singh, K.B., Foley, R.C., Onate-Sanchez, L., 2002. Transcription factors in plant defence and stress responses. Curr. Opin. Plant Biol. 5, 430–436.
Smayda, T., 1970. The suspension and sinking of phytoplankton in the sea. Oceanogr. Mar. Biol. Annu. Rev. 8, 67–74.
Smith, R.C., Stammerjohn, S.E., 2001. Variations of surface air temperature and sea ice extent in the Western Antarctic Peninsula (WAP) region. Ann. Glaciol. 33, 493–500.
Steig, E.J., Schneider, D.P., Rutherford, S.D., Mann, M.E., Comiso, J.C., Shindell, D.T., 2009. Warming of the Antarctic ice-sheet surface since the 1957 International Geophysical Year. Nature 457, 459–462.
Thessen, E., Dortch, Q., Parsons, M.L., Morrison, W., 2005. Effect of salinity on *Pseudo-nitzschia species* (Bacillarophyceae) growth and distribution. J. Phycol. 41, 21–29.
Treguer, P., Le Corre, P., 1975. Manuel d'analisis des sels nutritifs. Université de Bretagne Occidentale, Brest.
Utermöhl, H., 1958. Zur vervollkommnung der quantitativen phytoplankton-methodik. Mitt. Int. Ver. Theor. Angew. Limnol. 9, 1–38.
Van De Poll, W.H., Van Leeuwe, M.A., Roggeveld, J., Buma, A.G.J., 2005. Nutrient limitation and high irradiance acclimation reduce par and uv-induced viability loss in the Antarctic diatom Chaetoceros brevis (Bacillariophyceae). J. Phycol. 41, 840–850.
Vaughan, D.G., 2006. Recent trends in melting conditions on the Antarctic Peninsula and their implications for ice-sheet mass balance and sea level. Arct. Antarct. Alp. Res. 38, 147–152.
Vernet, M., Sines, K., Chakos, D., Cefarelli, A.O., Ekern, L., 2011. Impacts on phytoplankton dynamics by free-drifting icebergs in the NW Weddell Sea. Deep-Sea Res. II 58, 1422–1435.
Waite, A., Fisher, A., Thompson, P.A., Harrison, P.J., 1997. Sinking rate versus cell volume relationships illuminate sinking rate control mechanisms in marine diatoms. Mar. Ecol. Prog. Ser. 157, 97–108.
Zhu, J.K., 2002. Salt and drought stress signal transduction in plants. Annu. Rev. Plant Biol. 53, 247–273.